

Team LEYA in 10th ABAW Competition: Multimodal Ambivalence/Hesitancy Recognition Approach

Elena Ryumina

St. Petersburg Federal Research Center
of the Russian Academy of Sciences
St. Petersburg, Russia

ryumina.e@iiias.spb.su

Alexandr Axyonov

St. Petersburg Federal Research Center
of the Russian Academy of Sciences
St. Petersburg, Russia

axyonov.a@iiias.spb.su

Dmitry Sysoev

HSE University
St. Petersburg, Russia

dsysoev@hse.ru

Timur Abdulkadirov

HSE University
St. Petersburg, Russia

tnabdulkadirov@edu.hse.ru

Kirill Almetov

HSE University
St. Petersburg, Russia

koalmetov@edu.hse.ru

Yulia Morozova

HSE University
St. Petersburg, Russia

yuvmorozova_1@edu.hse.ru

Dmitry Ryumin

HSE University
St. Petersburg Federal Research Center
of the Russian Academy of Sciences
St. Petersburg, Russia

daryumin@hse.ru

Abstract

Ambivalence/hesitancy recognition in unconstrained videos is a challenging problem due to the subtle, multimodal, and context-dependent nature of this behavioral state. In this paper, a multimodal approach for video-level ambivalence/hesitancy recognition is presented for the 10th ABAW Competition. The proposed approach integrates four complementary modalities: scene, face, audio, and text. Scene dynamics are captured with a VideoMAE-based model, facial information is encoded through emotional frame-level embeddings aggregated by statistical pooling, acoustic representations are extracted with Emotion-Wav2Vec2.0 and processed by a Mamba-based temporal encoder, and linguistic cues are modeled using fine-tuned transformer-based text models. The resulting unimodal embeddings are further combined using multimodal fusion models, including prototype-augmented variants. Experiments on the BAH corpus demonstrate clear gains of multimodal fusion over all unimodal baselines. The best unimodal configuration achieved an average MF1 of 70.02%, whereas the best multimodal fusion model reached 83.25%. The highest final test performance, 71.43%, was obtained by an ensemble of five prototype-augmented fusion models. The obtained results highlight the importance of comple-

mentary multimodal cues and robust fusion strategies for ambivalence/hesitancy recognition. The source code is publicly available¹.

1. Introduction

Affective computing aims to endow intelligent systems with the ability to perceive, model, and interpret human affect from signals such as facial behavior [27], speech [11], language [5], and body motion [19]. This capability is important for human-computer interaction, digital health, education, and assistive technologies, where decisions often depend on subtle and context-dependent behavioral cues [23]. Within this area, the Ambivalence/Hesitancy (A/H) Video Recognition Challenge of the 10th Workshop and Competition on Affective & Behavior Analysis in-the-Wild (ABAW) focuses on a particularly difficult binary task: given a video, the goal is to predict whether it contains A/H or not at the video level [12].

A/H recognition is important because these states are strongly linked to decision uncertainty, resistance, and fluctuating motivation during behavior change. In digital behavioral health interventions, such signals can help identify

¹<https://github.com/LEYA-HSE/ABAW10-BAH>

whether a person is ready to change, struggling with conflicting intentions, or at risk of disengagement [3]. Unlike basic emotions (such as happiness, surprise), A/H is subtle and often manifests through inconsistencies across modalities, for example, between what a person says, how they say it, and how they look while speaking. This makes the task inherently multimodal and particularly challenging [12, 23].

González-González et al. [12] established baselines using visual facial information, audio, and speech transcripts, and showed that text was the best unimodal cue, while multimodal fusion could yield additional gains but required specialized designs to capture cross-modal inconsistencies characteristic of A/H. Similarly, Savchenko and Savchenko [29] explored face, audio, and text modalities, with the best validation result achieved by combining textual and facial features, whereas Hallmen et al. [14] used text, vision, and audio, and their best final Behavioural Ambivalence/Hesitancy (BAH) submission was based on trimodal fusion. Therefore, multimodal modeling remains a promising direction for A/H recognition, especially when modality interactions are explicitly taken into account and fusion preserves modality-specific cues under uncertainty or partially inconsistent multimodal evidence [9, 35].

This work proposes a multimodal approach that integrates audio, text, face, and scene information for video-level A/H recognition. First, a dedicated unimodal model is trained for each modality to learn compact modality-specific representations. The resulting modality embeddings are then projected into a shared latent space and fused by a Transformer-based multimodal module operating on modality tokens and augmented with a prototype-based classification objective. In this way, inter-modality dependencies are modeled directly at the video level, while the strengths of the specialized unimodal encoders are preserved for the final A/H prediction.

2. Related Work

González-González et al. [12] presented a broad benchmark suite including supervised unimodal, bimodal, and trimodal models based on facial video, audio, and speech transcripts, as well as zero-shot and personalization experiments. To study multimodal learning, they compared several fusion strategies, including concatenation-based fusion, co-attention, transformer-based fusion, and cross-attention fusion. Their results showed that text is the strongest unimodal cue, while effective A/H recognition requires specialized multimodal and temporal modeling to capture subtle inconsistencies across modalities.

Among the approaches proposed for the first public A/H challenge, Hallmen et al. [14] used a trimodal architecture combining text, vision, and audio. Their framework extracts visual features with a Vision Transformer (ViT) [4], audio representations with Wav2Vec 2.0 [2], and transcript em-

beddings with the Bidirectional Encoder Representations from Transformers (BERT) [7] text encoder, applies temporal modeling to the visual and audio streams with Long Short-Term Memorys (LSTMs) [16], and fuses the resulting modality-specific representations with an Multilayer Perceptron (MLP) [26]. Their analysis showed that text is the most informative modality. The best final BAH submission was obtained using trimodal fusion, which is consistent with recent studies [9, 20] indicating that preserving complementary modality-specific information during fusion improves multimodal prediction.

In contrast, Savchenko and Savchenko [29] used a lighter pipeline based on facial, acoustic, and textual features extracted with EmotiEffLib [30], Wav2Vec 2.0 [2], and RoBERTa-based [21] text representations. Audio and text features were aligned to the visual timeline by interpolation, and fusion was implemented either through early concatenation followed by a feed-forward classifier or through blending of unimodal predictions. In addition, a video-level logistic regression model over pooled text features was used as a filtering step. Their experiments again showed that text is the strongest unimodal modality, while the best validation result was achieved by combining text and facial information.

In summary, prior work shows that text is the strongest unimodal cue for A/H, while multimodal fusion remains beneficial, especially when it preserves complementary information across modalities and accounts for uncertainty in multimodal evidence. Unlike previous approaches, which mainly rely on face, audio, and text with relatively simple fusion schemes, our approach additionally incorporates scene information and uses a Transformer-based fusion module over modality-specific representations learned by dedicated unimodal models, further regularized by a prototype-based classification objective.

3. Proposed Approach

The overall pipeline of the proposed approach is shown in Figure 1. Our approach addresses multimodal A/H recognition by extracting complementary information from several synchronized modalities. The obtained representations are then aggregated and fused to produce the final prediction. The following subsections describe the main components of the proposed approach.

3.1. Scene-based Visual Model

To analyze behavioral dynamics and detect uncertainty, we employ the Video Masked Autoencoder (VideoMAE) architecture [32] based on the ViT [8] framework and pre-trained on the Kinetics-400 corpus [17]. For each video, $T_v = 16$ frames are uniformly sampled, resized to 224×224 , and normalized using ImageNet [6] statistics. The input video clip is processed using tubelet embedding, where it is parti-

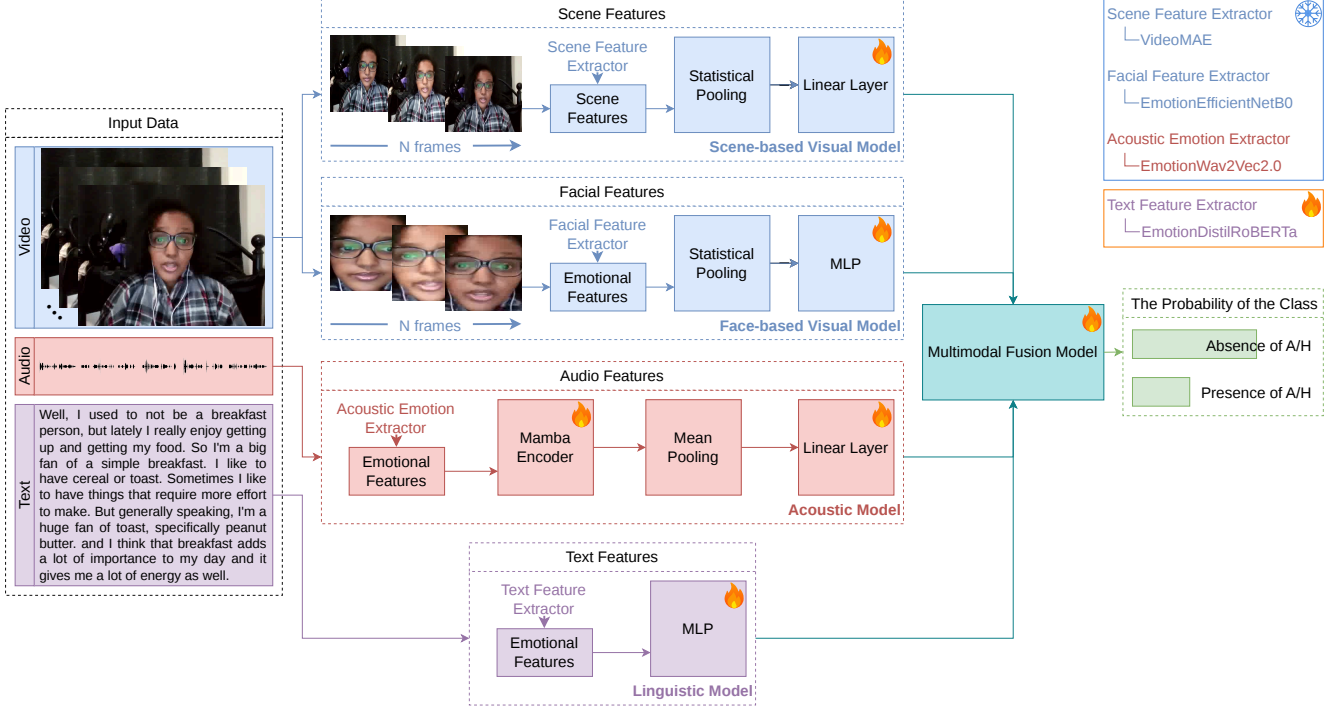


Figure 1. Pipeline of the proposed multimodal approach.

tioned into non-overlapping spatio-temporal patches of size $2 \times 16 \times 16$. These tubelets are projected into a $D = 768$ latent space and combined with learnable positional embeddings.

The resulting tokens are processed by a Transformer encoder with spatio-temporal self-attention to model spatio-temporal dependencies. A compact scene embedding h_s is obtained by applying global average pooling to the output tokens:

$$h_s = \frac{1}{N} \sum_{i=1}^N z_i, \quad (1)$$

where N is the number of output tokens and z_i denotes the representation of the i -th token.

3.2. Face-based Visual Model

For each video, frames are uniformly sampled, and a YOLO-based face detector² is applied to each sampled frame. When multiple faces are detected, the largest bounding box is selected. If no face is detected, the full frame is used as a fallback crop.

The cropped face is resized to 224×224 and normalized with ImageNet [6] statistics, then passed to an EfficientNetB0 [31] extractor fine-tuned on the AffectNet+ corpus [10], hereafter referred to as EmotionEfficientNetB0. The extractor produces one emotional embedding vector per

²<https://github.com/lindevs/yolov8-face>

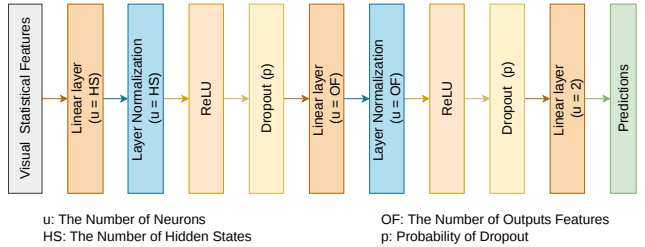


Figure 2. Visual MLP architecture.

sampled frame. No extra embedding normalization is applied.

For each video, frame-level embeddings $\{e_f\}_{f=1}^F$ are aggregated using statistical pooling:

$$\mu = \frac{1}{F} \sum_{f=1}^F e_f, \quad \sigma = \sqrt{\frac{1}{F} \sum_{f=1}^F (e_f - \mu)^2}. \quad (2)$$

The final face representation is formed by the concatenation $[\mu; \sigma]$. The resulting statistical representation is then used as input to an MLP, as shown in Figure 2.

3.3. Acoustic Model

For the audio modality, the audio track is extracted from each video and resampled to 16 kHz. A pre-trained

Wav2Vec2.0 model [34]³, fine-tuned on the MSP-Podcast corpus [22], is used to extract acoustic emotion features. For simplicity, this encoder is referred to as Emotion-Wav2Vec2.0.

As a result, each audio segment is represented as a sequence of embeddings of size $T_a \times 1024$, where T_a denotes the number of temporal steps and 1024 is the feature dimension. The value of T_a depends on the duration of the input video.

The extracted acoustic representations are then processed by a sequential encoder to model temporal dependencies in the speech signal. In the main configuration, the extracted acoustic representations are processed by a Mamba encoder [13], followed by mean pooling over the temporal dimension to obtain a compact acoustic embedding:

$$a = \frac{1}{T_a} \sum_{t=1}^{T_a} s_t, \quad (3)$$

where s_t denotes the representation at the t -th temporal step and a is the pooled acoustic embedding. The resulting embedding is then passed through a linear layer to produce the final prediction. In addition to the Mamba-based [13] variant, a Transformer-based [33] encoder was also evaluated as an alternative sequential architecture.

3.4. Linguistic Model

For the linguistic modality, all audio recordings are transcribed into text. These transcriptions were automatically extracted by the corpus authors [12].

Several text-based modeling strategies are considered. A classical Term Frequency-Inverse Document Frequency (TF-IDF) [28] representation is first used to encode the relative importance of words and phrases in each transcription. The resulting features are combined with conventional classifiers, including logistic regression and Gradient Boosting Machines (GBM) models such as LightGBM [18] and CatBoost [24].

Pre-trained transformer-based language models are also used to obtain contextualized text representations. EmotionDistilRoBERTa⁴, allMiniLM⁵, EmotionTextClassifier⁶, and DeBERTa [15] are used to encode the transcriptions into dense embeddings. Both the [CLS] token representation and mean pooling over token embeddings are explored, followed by a GBM-based classifier.

³<https://huggingface.co/audeering/wav2vec2-large-robust-12-ft-emotion-msp-dim>

⁴<https://huggingface.co/j-hartmann/emotion-english-distilroberta-base/>

⁵<https://huggingface.co/sentence-transformers/all-MiniLM-L6-v2>

⁶https://huggingface.co/michelleli99/emotion_text_classifier

In the main configuration, EmotionDistilRoBERTa is directly fine-tuned for A/H recognition. Its output representation is passed through an MLP-based classification head to produce the final prediction. Other fine-tuned transformer variants, including EmotionTextClassifier, are also evaluated.

3.5. Modality Fusion Model

A two-stage strategy is adopted. First, unimodal models for scene, face, audio, and text are trained independently on the target corpus. Then, for each video, one fixed-dimensional embedding per modality is extracted from the corresponding unimodal branch and used as input to the fusion model.

Let M be the number of modalities, $m \in \{1, \dots, M\}$ the modality index, and $x_m \in \mathbb{R}^{d_m}$ the input embedding of modality m , where d_m denotes its original dimensionality. Each modality is projected into a shared latent space \mathbb{R}^d :

$$u_m = \phi_m(x_m), \quad u_m \in \mathbb{R}^d, \quad (4)$$

where ϕ_m is a modality-specific projector composed of a linear layer, layer normalization, Gaussian Error Linear Unit (GELU), and dropout. The resulting modality tokens are stacked into a matrix:

$$U = [u_1; \dots; u_M] \in \mathbb{R}^{M \times d}. \quad (5)$$

If one or more modality embeddings are unavailable for a given sample, a binary modality mask is provided to the fusion encoder so that the corresponding tokens are masked out during self-attention. A learnable modality embedding matrix $E_{\text{mod}} \in \mathbb{R}^{M \times d}$ is added to the token sequence:

$$Z^{(0)} = U + E_{\text{mod}}, \quad (6)$$

where $Z^{(0)}$ is the input token sequence to the Transformer encoder.

The token sequence is processed by a stack of Transformer encoder layers:

$$Z^{(l+1)} = T^{(l)}(Z^{(l)}), \quad l = 0, \dots, L-1, \quad (7)$$

where $T^{(l)}(\cdot)$ denotes the l -th Transformer encoder block and L is the number of layers. The final fused representation is obtained by masked mean pooling over the output modality tokens:

$$z_{\text{fused}} = \frac{\sum_{m=1}^M \mu_m z_m^{(L)}}{\sum_{m=1}^M \mu_m}, \quad (8)$$

where $z_m^{(L)}$ denotes the output representation of modality m at the last encoder layer and $\mu_m \in \{0, 1\}$ indicates whether modality m is available for the given sample.

For the prototype-augmented variant, the fused representation is compared with a set of learnable class-specific prototypes. Let $P_c = \{p_{c,k}\}_{k=1}^K$ be the prototype set for class

c , where K is the number of prototypes per class. The similarity score for class c is computed as:

$$\hat{y}_c^{\text{proto}} = \log \sum_{k=1}^K \exp \left(\frac{\tilde{z}_{\text{fused}}^\top \tilde{p}_{c,k}}{\tau} \right), \quad (9)$$

where \tilde{z}_{fused} and $\tilde{p}_{c,k}$ denote the ℓ_2 -normalized fused representation and class prototypes, respectively, and τ is a temperature parameter. In the implemented model, the prototype head does not directly produce the final multimodal prediction; instead, it contributes an auxiliary loss term during training, while the final output logits are produced by the main linear classifier.

Accordingly, the overall training objective is defined as:

$$\mathcal{L} = \mathcal{L}_{\text{cls}} + \lambda_{\text{proto}} \mathcal{L}_{\text{proto}} + \lambda_{\text{div}} \mathcal{L}_{\text{div}}, \quad (10)$$

where \mathcal{L}_{cls} is the main classification loss computed from the output logits of the linear classifier, $\mathcal{L}_{\text{proto}}$ is the auxiliary classification loss computed from the prototype-based logits, and \mathcal{L}_{div} is the prototype diversity regularization term.

4. Experiments

4.1. Research Corpus

The BAH corpus is the core research corpus for the 10th ABAW A/H challenge. It was collected to support multimodal recognition of ambivalence and hesitancy in videos recorded in a realistic digital behavior change scenario [12]. Participants answered a predefined set of questions designed to elicit neutral, positive, negative, willing, resistant, ambivalent, and hesitant responses. The data were collected through an online platform with an avatar-guided interaction setup in order to mimic real-world personalized behavioral interventions [12].

The full corpus contains 1,427 videos from 300 participants, totaling 10.60 hours of recordings. It includes video-level and frame-level expert annotations, timestamps of A/H segments, cropped and aligned faces, speech transcripts with timestamps, and participant metadata [12]. Since ambivalence and hesitancy are difficult to separate reliably in practice, the task is formulated as a binary classification problem indicating the presence or absence of A/H [12]. For the 10th ABAW A/H challenge, the corpus is partitioned participant-wise into training, validation, public test, and private test subsets. Video-level prediction is evaluated using Macro F1-score (MF1) as the main metric.

4.2. Experimental Setup

During the development of the unimodal models, several alternative configurations were evaluated. Scene modeling was performed using 16-frame sequences resized to 224×224 , trained for 15 epochs with AdamW, a Learning Rate (LR) of $2e-5$, weight decay of $1e-2$, batch size 4,

cosine annealing, and Label Smoothing (LS) of 0.1. For the face-based visual modality, both statistical features with an MLP and raw embeddings extracted by ViT [8] and Contrastive Language-Image Pretraining (CLIP) [25] in combination with Transformer [33] and Mamba [13] encoders were considered. The best configuration was based on statistical features with an MLP. A grid search over the number of frames, hidden states, output features, LR, and optimizer selected a setup with 30 frames, 16 hidden states, 256 output features, a LR of $1e-3$, and AdamW.

For the acoustic modality, embeddings from different EmotionWav2Vec2.0 layers and different temporal encoders, including Mamba and Transformer, were evaluated. The best result was obtained with layer 10 and Mamba. In all primary runs, AdamW was used. The selected acoustic setup employed hidden size 256, feed-forward size 512, dropout 0.1, mean pooling, Mamba state size 8, convolution kernel size 4, and expansion factor 2. In the linguistic modality, TF-IDF features were evaluated with vocabulary sizes from 100 to 10,000 and n -grams from unigrams to trigrams, with hyperparameter tuning for Logistic Regression and GBM models. Transformer-based text models were also fine-tuned using partially frozen backbones and jointly trained MLP heads. The number of hidden layers varied from 1 to 3, the hidden size from 64 to 128, and dropout from 0 to 0.3. AdamW and Stochastic Gradient Descent (SGD) were explored, the LR was searched in the range from $1e-5$ to 0.1, the batch size was set to 16, and training lasted from 3 to 20 epochs with early stopping.

Multimodal fusion was performed using embeddings extracted from the selected scene, face, audio, and text models. Both non-prototype and prototype-augmented variants were evaluated, and the final system was based on the prototype-augmented fusion model operating on embedding-level inputs. To reduce sensitivity to random initialization, model selection relied on a stability-oriented hyperparameter search with Optuna [1] using five fixed random seeds: 42, 2025, 7777, 12345, and 31415. Each candidate configuration was trained and evaluated five times, and the final score was computed as the average MF1 across these runs. The selected fusion model used a shared latent dimensionality of 128, 6 Transformer encoder layers, 4 attention heads, a feed-forward expansion factor of 6, no [CLS] token, and dropout of 0.45. The prototype head used 16 learnable prototypes per class with temperature $\tau = 0.3$. Training was performed with RMSprop, a LR of $9.44e-5$, weight decay of $5.55e-4$, LS of 0.02, gradient clipping of 0.5, and a cosine learning-rate scheduler. The prototype loss weight was set to $\lambda_{\text{proto}} = 0.2$, while the diversity regularization term was disabled, i.e., $\lambda_{\text{div}} = 0$. Final predictions were obtained by averaging the class probabilities of the 5 seed-specific models.

| ID | Model Configuration | | | BAH sub-corpus | | | |
|----------------|--------------------------|---|---------------------|--------------------------|---------------|------------------|---------------------|
| | Modality | Features | Classifier | Devel. / Valid. (MF1, %) | Test (MF1, %) | Average (MF1, %) | Final test (MF1, %) |
| 1 | Face | EmotionEfficientNetB0 + Statistical Features | MLP | 65.29 | 60.05 | 62.67 | - |
| 2 | Scene | VideoMAE | Linear Layer | 61.71 | 62.21 | 61.96 | - |
| 3 | Audio | EmotionWav2Vec2.0 + Mamba | Linear Layer | 67.20 | 70.87 | 69.03 | - |
| 4 | Text | TF-IDF | Logistic Regression | 68.30 | 67.75 | 68.03 | - |
| 5 | Text | TF-IDF | CatBoost | 65.56 | 72.02 | 68.79 | - |
| 6 | Text | Fine-tuned EmotionTextClassifier | MLP | 69.28 | 70.72 | 70.00 | - |
| 7 | Text | Fine-tuned EmotionDistilRoBERTa | MLP | 68.54 | 71.49 | 70.02 | - |
| 8 | Models IDs 1, 2, 3 and 4 | Multimodal Fusion Model | Linear Layer | 80.79 | 77.03 | 78.91 | - |
| 9 | Models IDs 1, 2, 3 and 5 | Multimodal Fusion Model | Linear Layer | 77.91 | 78.54 | 78.22 | - |
| 10 | Models IDs 1, 2, 3 and 6 | Multimodal Fusion Model | Linear Layer | 78.35 | 77.03 | 77.69 | - |
| 11 | Models IDs 1, 2, 3 and 7 | Multimodal Fusion Model | Linear Layer | 85.38 | 79.94 | 82.66 | 68.32 |
| 12 | Models IDs 1, 2, 3 and 7 | Multimodal Fusion Model with Prototype Head | Linear Layer | 83.79 | 82.72 | 83.25 | 65.21 |
| 13 | Models IDs 1, 2, 3 and 7 | Ensemble of Five Multimodal Fusion Models | Linear Layer | 81.94 | 80.64 | 81.29 | 70.17 |
| 14 | Models IDs 1, 2, 3 and 7 | Ensemble of Five Multimodal Fusion Models with Prototype Head | Linear Layer | 83.00 | 80.77 | 81.89 | 71.43 |
| Ablation Study | | | | | | | |
| 15 | Models IDs 1 and 3 | Multimodal Fusion Model | Linear Layer | 63.36 | 71.44 | 67.40 | - |
| 16 | Models IDs 1 and 7 | Multimodal Fusion Model | Linear Layer | 65.29 | 61.19 | 63.24 | - |
| 17 | Models IDs 1 and 2 | Multimodal Fusion Model | Linear Layer | 78.07 | 77.09 | 77.58 | - |
| 18 | Models IDs 3 and 7 | Multimodal Fusion Model | Linear Layer | 67.05 | 70.99 | 69.02 | - |
| 19 | Models IDs 2 and 3 | Multimodal Fusion Model | Linear Layer | 77.37 | 77.66 | 77.51 | - |
| 20 | Models IDs 2 and 7 | Multimodal Fusion Model | Linear Layer | 81.77 | 79.00 | 80.39 | - |
| 21 | Models IDs 2, 3 and 7 | Multimodal Fusion Model | Linear Layer | 79.89 | 77.63 | 78.76 | - |
| 22 | Models IDs 1, 2 and 7 | Multimodal Fusion Model | Linear Layer | 79.89 | 77.65 | 78.77 | - |
| 23 | Models IDs 1, 2 and 3 | Multimodal Fusion Model | Linear Layer | 76.10 | 79.15 | 77.62 | - |
| 24 | Models IDs 1, 3 and 7 | Multimodal Fusion Model | Linear Layer | 68.08 | 70.41 | 69.25 | - |

Table 1. Experimental results on the BAH corpus for video-level A/H recognition.

4.3. Experimental Results

The experimental results are presented in Table 1. Among the unimodal models, the best average MF1 was obtained by the fine-tuned EmotionDistilRoBERTa model (70.02%), followed closely by the fine-tuned EmotionTextClassifier (70.00%) and the acoustic model based on EmotionWav2Vec2.0 and Mamba (69.03%). The TF-IDF-based text models also showed competitive results, reaching 68.03% with Logistic Regression and 68.79% with CatBoost. In contrast, the face- and scene-based models achieved lower average scores of 62.67% and 61.96%, respectively.

All multimodal fusion models outperformed the unimodal baselines. Among the single fusion models, the best average result was achieved by the prototype-augmented fusion model based on the selected scene, face, audio, and text modalities (ID 12), with 83.25%, while the corresponding fusion model without the prototype head (ID 11) reached 82.66%. These results indicate that both multimodal integration and prototype-based classification are beneficial under the development and public test settings.

The final test results show a different trend. Among the submitted four-modality systems, the best performance was obtained by the ensemble of five prototype-augmented fusion models (ID 14), which achieved 71.43%. The ensemble of five fusion models without the prototype head (ID 13) reached 70.17%, while the single fusion models achieved 68.32% (ID 11) and 65.21% (ID 12). Thus, although the prototype-augmented single model achieved the highest average result, ensembling was essential for the strongest final test performance and improved robustness on the private evaluation split.

The ablation study further confirms the benefit of com-

binning modalities. The strongest two-modality result was obtained by combining scene and text features (ID 20), with an average MF1 of 80.39%. Among the three-modality settings, the best performance was achieved by combining face, scene, and text features (ID 22), with 78.77%. Overall, the best results were obtained with four-modality fusion.

5. Conclusions

This paper presented a multimodal approach for video-level A/H recognition on the BAH corpus. The proposed approach combined scene, face, audio, and text modalities and consistently outperformed unimodal baselines. Among the unimodal models, the best average MF1 of 70.02% was achieved by the fine-tuned EmotionDistilRoBERTa model, confirming the strong contribution of the linguistic modality. At the multimodal level, the best average result of 83.25% was obtained by the prototype-augmented fusion model, while the best final test performance of 71.43% was achieved by the ensemble of five prototype-augmented fusion models.

The ablation study showed that scene and text provide the strongest complementary signal among modality pairs, and that extending the fusion scheme to all four modalities yields the most effective overall solution. The comparison between single fusion models and their ensembles further indicates that robust model aggregation is important for generalization on the private test split. Overall, these results demonstrate that prototype-augmented multimodal fusion is an effective and robust strategy for A/H recognition in unconstrained videos.

References

- [1] Takuya Akiba, Shotaro Sano, Toshihiko Yanase, Takeru Ohta, and Masanori Koyama. Optuna: A next-generation hyperparameter optimization framework. In *KDD*, pages 2623–2631, 2019. 5
- [2] Alexei Baevski, Yuhao Zhou, Abdelrahman Mohamed, and Michael Auli. Wav2vec 2.0: A framework for self-supervised learning of speech representations. In *NeurIPS*, pages 12449–12460, 2020. 2
- [3] Laura E Bijkerk, Mark Spigt, Anke Oenema, and Nicole Geschwind. Engagement with mental health and health behavior change interventions: an integrative review of key concepts. *J. Context. Behav. Sci.*, 32:1–14, 2024. 2
- [4] Mathilde Caron, Hugo Touvron, Ishan Misra, Hervé Jégou, Julien Mairal, Piotr Bojanowski, and Armand Joulin. Emerging properties in self-supervised vision transformers. In *ICCV*, pages 9650–9660, 2021. 2
- [5] Jiawen Deng and Fuji Ren. A survey of textual emotion recognition and its challenges. *IEEE Trans. Affect. Comput.*, 14(1):49–67, 2021. 1
- [6] Jia Deng, Wei Dong, Richard Socher, Li-Jia Li, Kai Li, and Li Fei-Fei. Imagenet: A large-scale hierarchical image database. In *CVPR*, pages 248–255, 2009. 2, 3
- [7] Jacob Devlin, Ming-Wei Chang, Kenton Lee, and Kristina Toutanova. Bert: Pre-training of deep bidirectional transformers for language understanding. In *NAACL*, pages 4171–4186, 2019. 2
- [8] Alexey Dosovitskiy, Lucas Beyer, Alexander Kolesnikov, Dirk Weissenborn, Xiaohua Zhai, Thomas Unterthiner, Mostafa Dehghani, Matthias Minderer, Georg Heigold, Sylvain Gelly, et al. An image is worth 16x16 words: Transformers for image recognition at scale. In *ICLR*, pages 1–22, 2021. 2, 5
- [9] Yiyang Fang, Wenke Huang, Guancheng Wan, Kehua Su, and Mang Ye. Emoe: Modality-specific enhanced dynamic emotion experts. In *CVPR*, pages 14314–14324, 2025. 2
- [10] Ali Pourramezan Fard, Mohammad Mehdi Hosseini, Timothy D Sweeny, and Mohammad H Mahoor. Affectnet+: A database for enhancing facial expression recognition with soft-labels. *IEEE Trans. Affect. Comput.*, 17:784–800, 2026. 3
- [11] Swapna Mol George and P Muhamed Ilyas. A review on speech emotion recognition: A survey, recent advances, challenges, and the influence of noise. *Neurocomputing*, 568: 1–23, 2024. 1
- [12] Manuela González-González, Soufiane Belharbi, Muhammad Osama Zeeshan, Masoumeh Sharafi, Muhammad Haseeb Aslam, Marco Pedersoli, Alessandro Lameiras Koerich, Simon L Bacon, and Eric Granger. Bah dataset for ambivalence/hesitancy recognition in videos for digital behavioural change. In *ICLR*, pages 1–17, 2026. 1, 2, 4, 5
- [13] Albert Gu and Tri Dao. Mamba: Linear-time sequence modeling with selective state spaces. In *CoLM*, pages 1–16, 2024. 4, 5
- [14] Tobias Hallmen, Robin-Nico Kampa, Fabian Deuser, Norbert Oswald, and Elisabeth André. Semantic matters: Multimodal features for affective analysis. In *CVPRW*, pages 5761–5770, 2025. 2
- [15] Pengcheng He, Xiaodong Liu, Jianfeng Gao, and Weizhu Chen. DeBERTa: Decoding-enhanced bert with disentangled attention. In *ICLR*, pages 1–21, 2021. 4
- [16] Sepp Hochreiter and Jürgen Schmidhuber. Long short-term memory. *Neural Comput.*, 9(8):1735–1780, 1997. 2
- [17] Will Kay, Joao Carreira, Karen Simonyan, Brian Zhang, Chloe Hillier, Sudheendra Vijayanarasimhan, Fabio Viola, Tim Green, Trevor Back, Paul Natsev, Mustafa Suleyman, and Andrew Zisserman. The kinetics human action video dataset. *arXiv preprint arXiv:1705.06950*, pages 1–22, 2017. 2
- [18] Guolin Ke, Qi Meng, Thomas Finley, Taifeng Wang, Wei Chen, Weidong Ma, Qiwei Ye, and Tie-Yan Liu. Lightgbm: A highly efficient gradient boosting decision tree. In *NeurIPS*, pages 1–9, 2017. 4
- [19] Sze Chit Leong, Yuk Ming Tang, Chung Hin Lai, and Carmen Ka Man Lee. Facial expression and body gesture emotion recognition: A systematic review on the use of visual data in affective computing. *Comput. Sci. Rev.*, 48:1–13, 2023. 1
- [20] Chenxin Li, Yifan Liu, Panwang Pan, Hengyu Liu, Xinyu Liu, Wuyang Li, Cheng Wang, Weihao Yu, Yiyang Lin, and Yixuan Yuan. Infobridge: Balanced multimodal integration through conditional dependency modeling. In *ICCV*, pages 393–404, 2025. 2
- [21] Yinhan Liu, Myle Ott, Naman Goyal, Jingfei Du, Mandar Joshi, Danqi Chen, Omer Levy, Mike Lewis, Luke Zettlemoyer, and Veselin Stoyanov. Roberta: A robustly optimized bert pretraining approach. *arXiv preprint arXiv:1907.11692*, 2019. 2
- [22] Reza Lotfian and Carlos Busso. Building naturalistic emotionally balanced speech corpus by retrieving emotional speech from existing podcast recordings. *IEEE Trans. Affect. Comput.*, 10(4):471–483, 2017. 4
- [23] Soujanya Poria, Erik Cambria, Rajiv Bajpai, and Amir Hussain. A review of affective computing: From unimodal analysis to multimodal fusion. *Inf. Fusion*, 37:98–125, 2017. 1, 2
- [24] Liudmila Prokhorenkova, Gleb Gusev, Aleksandr Vorobev, Anna Veronika Dorogush, and Andrey Gulin. Catboost: unbiased boosting with categorical features. In *NeurIPS*, pages 1–11, 2018. 4
- [25] Alec Radford, Jong Wook Kim, Chris Hallacy, Aditya Ramesh, Gabriel Goh, Sandhini Agarwal, Girish Sastry, Amanda Askell, Pamela Mishkin, Jack Clark, Gretchen Krueger, and Ilya Sutskever. Learning transferable visual models from natural language supervision. In *ICML*, pages 8748–8763, 2021. 5
- [26] David E Rumelhart, Geoffrey E Hinton, and Ronald J Williams. Learning representations by back-propagating errors. *Nature*, 323(6088):533–536, 1986. 2
- [27] Muhammad Sajjad, Fath U Min Ullah, Mohib Ullah, Georgia Christodoulou, Faouzi Alaya Cheikh, Mohammad Hiji, Khan Muhammad, and Joel JPC Rodrigues. A comprehensive survey on deep facial expression recognition: chal-

- lenges, applications, and future guidelines. *Alex. Eng. J.*, 68: 817–840, 2023. 1
- [28] G. Salton, A. Wong, and C. S. Yang. A vector space model for automatic indexing. *Commun. ACM*, 18(11):613–620, 1975. 4
- [29] Andrey Savchenko and Lyudmila Savchenko. Leveraging lightweight facial models and textual modality in audio-visual emotional understanding in-the-wild. In *CVPRW*, pages 5824–5834, 2025. 2
- [30] Andrey V Savchenko and Anna P Sidorova. Emotieffnet and temporal convolutional networks in video-based facial expression recognition and action unit detection. In *CVPRW*, pages 4849–4859, 2024. 2
- [31] Mingxing Tan and Quoc Le. Efficientnet: Rethinking model scaling for convolutional neural networks. In *ICML*, pages 6105–6114, 2019. 3
- [32] Zhan Tong, Yibing Song, Jue Wang, and Limin Wang. Videomae: Masked autoencoders are data-efficient learners for self-supervised video pre-training. In *NeurIPS*, pages 1–15, 2022. 2
- [33] Ashish Vaswani, Noam Shazeer, Niki Parmar, Jakob Uszkoreit, Llion Jones, Aidan N Gomez, Łukasz Kaiser, and Illia Polosukhin. Attention is all you need. In *NeurIPS*, pages 1–11, 2017. 4, 5
- [34] Johannes Wagner, Andreas Triantafyllopoulos, Hagen Wierstorf, Maximilian Schmitt, Felix Burkhardt, Florian Eyben, and Björn W. Schuller. Dawn of the transformer era in speech emotion recognition: Closing the valence gap. *IEEE Trans. Pattern Anal. Mach. Intell.*, pages 10745–10759, 2023. 4
- [35] Qu Yang, Qinghongya Shi, Tongxin Wang, and Mang Ye. Uncertain multimodal intention and emotion understanding in the wild. In *CVPR*, pages 24700–24709, 2025. 2